ELSEVIER

Journal of Alloys and Compounds 444–445 (2007) 114–118

Journal of ALLOYS AND COMPOUNDS

www.elsevier.com/locate/jallcom

Single crystal growth, superconductivity and Fermi surface study of plutonium compounds

Y. Haga [a,*], D. Aoki [b], H. Yamagami [c], T.D. Matsuda [a], K. Nakajima [d], Y. Arai [d], E. Yamamoto [a], A. Nakamura [a], Y. Homma [b], Y. Shiokawa [a,b], Y. Ōnuki [a,e]

[a] *Advanced Science Research Center, Japan Atomic Energy Agency, Tokai, Ibaraki 319-1195, Japan*
[b] *Institute for Materials Research, Tohoku University, Oarai, Ibaraki 311-1313, Japan*
[c] *Department of Physics, Faculty of Science, Kyoto Sangyo University, Kyoto 603-8555, Japan*
[d] *Nuclear Science and Engineering Directorate, Japan Atomic Energy Agency, Tokai, Ibaraki 319-1195, Japan*
[e] *Graduate School of Science, Osaka University, Toyonaka, Osaka 560-0043, Japan*

Received 17 August 2006; received in revised form 25 November 2006; accepted 27 November 2006
Available online 26 February 2007

Abstract

Single crystals of plutonium compounds $PuRhGa_5$ and $PuIn_3$ are successfully grown. For $PuRhGa_5$, anisotropy of the superconducting upper critical field was found and analyzed by the anisotropic mass model, consistent with quasi-two-dimensional electronic states predicted by band calculations. On the other hand, the de Haas–van Alphen oscillation was observed in $PuIn_3$. By comparing with the band calculations, it is concluded that 5f electrons are itinerant in $PuIn_3$.

Keywords: $PuRhGa_5$; $PuIn_3$; Fermi surface; Superconductivity

1. Introduction

The discovery of the superconductivity in plutonium compounds $PuCoGa_5$ [1] and $PuRhGa_5$ [2] has attracted attention because of their high-superconducting transition temperature T_c and possible magnetically mediated superconductivity inferred from several experimental results such as Curie–Weiss behavior in magnetic susceptibility, large specific heat jump and existence of line-nodes on the superconducting gap [1,3,4], similar to the isostructural heavy fermion superconductor $CeCoIn_5$ [5].

Existence of the quasi-two-dimensional Fermi surfaces in $PuCoGa_5$ is predicted by the band calculations based on the itinerant 5f electron picture, which might explain high T_c in this compound [6,7].

In the actinide compounds, the 5f-itinerant band model was successfully applied to many U compounds[8]. Such itinerant characteristics, observed in the U and Np compounds, might not be valid in heavy actinides. The wave function of 5f electrons of actinide metals shrinks with increasing the number of 5f electrons. Namely, the Wigner–Seitz radius steeply decreases from Th to Np as in transition metals, has a minimum in Np, and increases with further increase in the number of 5f electrons[9]. The Wigner–Seitz radius of Am is close to the localized 4f-electron radius, and thus the radius of Pu has an intermediate value between those of Np with the 5f-itinerant nature and Am with the 5f-localized nature.

In this paper, we present the anisotropic superconducting properties of $PuRhGa_5$ and the itinerant 5f electronic states observed in $PuIn_3$.

2. Experimental

Single crystals of $PuRhGa_5$ and $PuIn_3$ were grown by the Ga- and In-flux methods, respectively [10,11]. All the sample preparations were performed in argon-circulated glove boxes to avoid the oxidization of Pu metal. In the present study 94% enriched ^{239}Pu metal was used. The starting materials as well as excess flux were inserted into an alumina crucible. It was then put into a tungsten-heater furnace in argon atmosphere. The crucible was heated up to 1100 °C, maintained at that temperature for 2 h and then slowly cooled to room temperature over 12 h. Large single crystals with typical dimensions of 2.5 mm × 1.5 mm × 0.9 mm were then extracted from the melt. The

* Corresponding author. Tel.: +81 29 282 6735; fax: +81 29 282 5939.
E-mail address: haga.yoshinori@jaea.go.jp (Y. Haga).

0925-8388/$ – see front matter © 2006 Elsevier B.V. All rights reserved.
doi:10.1016/j.jallcom.2006.11.206

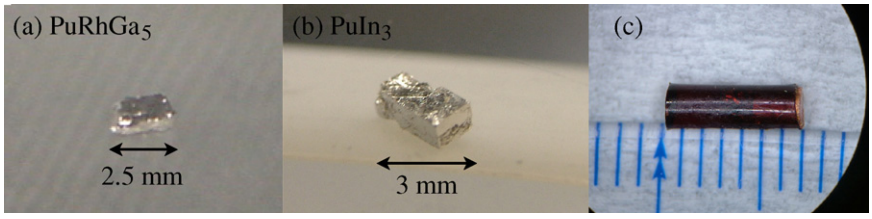

Fig. 1. Single crystals of (a) $PuRhGa_5$ and (b) $PuIn_3$ used for present study, and (c) encapsulation.

lattice parameter as well as the orientation of the single crystal sample were determined by the X-ray diffraction method, where the lattice parameters agree with the reported values.

Fig. 1 shows single crystals of $PuRhGa_5$ and $PuIn_3$ used in the present study.

In order to perform the low-temperature experiments, special care was taken in cooling the radioactive sample, where the self-heating effect due to the α-decay was 6.9 μW for the present $PuRhGa_5$ sample of 16.3 mg. In order to attain good thermal contact between the sample and the cryostat, the sample was fixed on a copper or silver disk which directly contacts with ^3He–^4He mixture. With this setup, the temperature deference between the sample and the mixture is estimated to be about 10 mK at the base temperature of 30 mK. It was inserted into a polyimide tube and filled with stycast epoxy. The magnetization was measured using a commercial SQUID magnetometer up to 55 kOe (Quantum Design MPMS-5). The ac susceptibility and dHvA measurements were performed using the field modulation technique under high magnetic fields up to 150 kOe in a dilution refregerator.

3. Superconducting properties of $PuRhGa_5$

Fig. 2 shows the temperature dependence of the inverse magnetic susceptibility χ for the magnetic field along the [1 0 0] and [0 0 1] directions. Both measurements were performed on the same sample, where the direction of the magnetic field was changed by rotating the sample tube around its axis, in order to minimize the anisotropy of back ground. Here we note that the background susceptibility due to the sample holder was almost independent of temperature, and was subtracted from the experimental data.

The susceptibility increases with decreasing temperature, but clearly includes a large value of the temperature-independent term χ_0. Namely, the susceptibility is expressed as $\chi = \chi_0 + C/(T + \theta_p)$, where $\chi_0 = 4.3 \times 10^{-4}$ and 4.5×10^{-4} emu/mol for $H \parallel [1\,0\,0]$ and [0 0 1], respectively. From the Curie term, we obtain an effective magnetic moment $\mu_{eff} = 0.85\mu_B$/Pu above 100 K for both directions, which is approximately equal to the free ion value of Pu^{3+}, as shown by solid lines in Fig. 1. It is not clear at present whether 5f electrons are localized at high temperatures. It is most likely necessary to measure the susceptibility at much higher temperatures. Below 100 K, the susceptibility deviates from the Curie–Weiss law, indicating a smaller effective moment.

An important finding in Fig. 2 is that anisotropy of the magnetic susceptibility is very small, which contrasts with relatively large anisotropy of the susceptibility in $CeCoIn_5$ [12]. The steep drop of the susceptibility below about 9 K, shown in Fig. 2, is due to superconductivity.

Fig. 3 shows the temperature dependence of ac susceptibility at 1 and 50 kOe for $H \parallel [1\,0\,0]$. The magnetization and ac susceptibility decrease below $T_c = 8.6$ K at 1 kOe, as shown by an arrow, at which the superconducting transition temperature is defined. The transition temperature shifts to a lower temperature $T_c = 7.0$ K at 50 kOe, as shown by the arrow.

We also carried out these measurements for $H \parallel [0\,0\,1]$. Fig. 3 shows the temperature dependence of the upper critical field H_{c2}. The slope of H_{c2} at T_c, $-dH_{c2}/dT$, is obtained as $-dH_{c2}/dT = 35$ and 20 kOe/K for $H \parallel [1\,0\,0]$ and [0 0 1], respectively.

To further clarify the anisotropy of the upper critical field, we measured the angular dependence of H_{c2} at 5 K by rotating

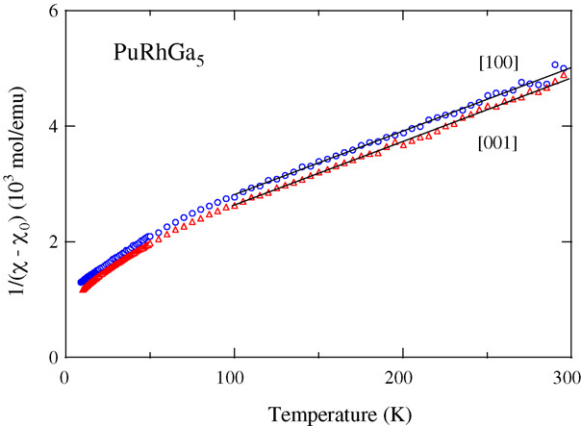

Fig. 2. Temperature dependences of inverse magnetic susceptibility of $PuRhGa_5$.

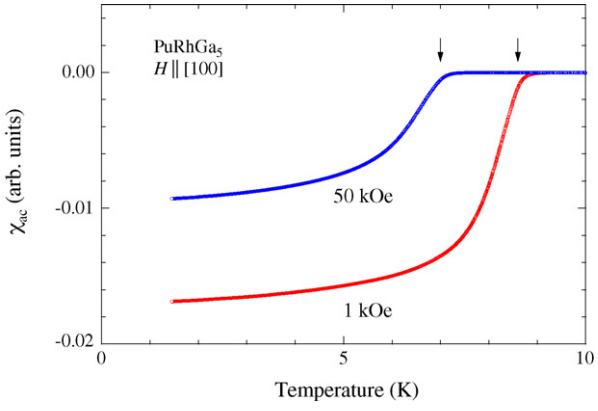

Fig. 3. Temperature dependences of ac susceptibility of $PuRhGa_5$ at 1 and 50 kOe along [1 0 0].

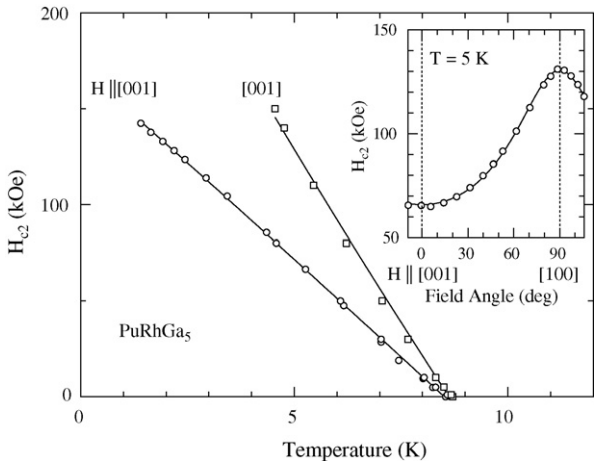

Fig. 4. Temperature dependence of upper critical field H_{c2} in $PuRhGa_5$. Solid lines indicate guidelines. Inset: angular dependence of H_{c2} at 5 K.

the sample, as shown in the inset of Fig. 4. Large anisotropy is observed: $H_{c2} = 130$ kOe for $H \parallel [1\,0\,0]$ and 66 kOe T for $H \parallel [0\,0\,1]$ at 5 K. This field dependence is well described by the anisotropic mass model. The solid line in Fig. 4 is the result of fitting using the following function [13]:

$$H_{c2}(\theta) = \frac{H_{c2}(\theta = 90^\circ)}{\sqrt{\sin^2\theta + (m_c^*/m_a^*)\cos^2\theta}}, \quad (1)$$

where m_c^*/m_a^* is the mass anisotropy ratio for the [0 0 1] (c) and [1 0 0] (a) directions, and θ is the field angle measured from [0 0 1] to [1 0 0]. $m_c^*/m_a^* = 3.9$ is similar to $m_c^*/m_a^* = 5.6$ obtained for $CeCoIn_5$ [14]. The quasi-two dimensional characteristics of the Fermi surfaces [6,7] are most likely reflected in anisotropy of the upper critical field, as in $CeCoIn_5$ [14]. To confirm this point, Fermi surface studies by means of dHvA experiment are desired.

From the anisotropy of H_{c2}, the quasi-two-dimensional electronic state is most likely realized in $PuRhGa_5$, as in $CeCoIn_5$. Using the present sample, the ^{69}Ga-NQR spin-lattice relaxation rate $1/T_1$ was measured recently, indicating no coherent peak at T_c and following a T^3-dependence below T_c, which results in an unconventional superconductor with a line node [4].

4. Fermi surfaces of $PuIn_3$

As mentioned above, quasi-two-dimensional Fermi surfaces are expected for $PuTGa_5$. Our first attempt to observe dHvA oscillations to confirm this point was, however, unsuccessful because of its high superconducting upper critical field: dHvA amplitudes generally significantly diminish in the superconducting mixed state.

We have succeeded in observing dHvA effect in a cubic $AuCu_3$-type plutonium compound $PuIn_3$ [11]. $PuIn_3$ is expected to be iso-electronic to a hypothetical reference compound "cubic-$PuGa_3$" of $PuTGa_5$, because the crystal structure of $PuTGa_5$ consists of a stacking of $PuGa_3$ and TGa_2 layers. However, "cubic-$PuGa_3$" is not stable but crystalizes in either hexagonal (low-temperature phase) or trigonal (high-temperature phase) structure [15].

$PuIn_3$ is reported as a paramagnetic with an enhanced electronic specific heat coefficient of about 100 mJ/K^2 mol. Recent photoemission studies for this compound revealed a 5f component near the Fermi energy [16].

We carried out the dHvA experiment for magnetic fields in both {1 0 0} and {1 1 0} planes, but the dHvA signal was observed only around the ⟨1 1 1⟩ direction. Fig. 5 shows the typical dHvA oscillations for the magnetic field tilted by 64° from ⟨1 0 0⟩ to ⟨1 1 0⟩ in the {1 1 0} plane and their fast-Fourier-transformed (FFT) spectra at 30 mK. Two sets of experiments, Ex 1 and Ex 2, were performed, where Ex 2 was carried out 9 days after Ex 1.

Two kinds of dHvA frequencies were observed: $F = 2.1 \times 10^7$ Oe named γ and $F = 5.5 \times 10^6$ Oe, where the dHvA frequency $F(= c\hbar S_F/2\pi e)$ is proportional to the extremal (maximum or minimum) cross-sectional area of the Fermi surface S_F. The dHvA amplitude of branch γ is extremely reduced as a function of time, namely at Ex 2, which is due to point defects produced by α-decay of ^{239}Pu [17]. One α-decay event produces an α particle and a ^{235}U recoil atom. The latter makes 2200 Frenkel-type defects per event, causing a severe scattering of conduction electrons. Although 90% of those defects recovers due to lattice vibrations at room temperature, they are accumulated at low temperatures. On the other hand, the dHvA amplitude of $F = 5.5 \times 10^6$ Oe is approximately the same between Ex 1 and Ex 2, being unaffected by the radiation damage. The angular dependence of the dHvA frequency of this branch does

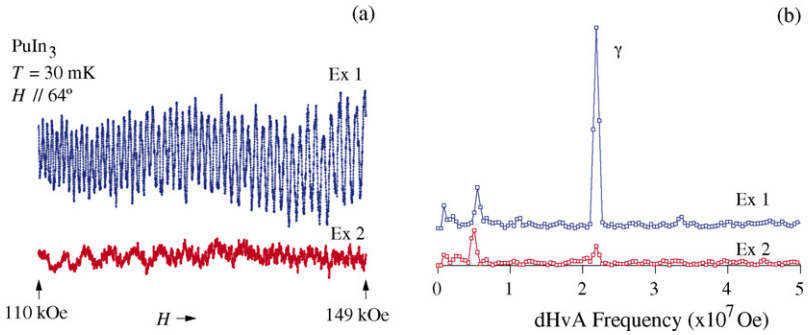

Fig. 5. Two kinds of dHvA experiments Ex 1 and Ex 2, and their FFT spectra in $PuIn_3$ for magnetic field tilted by 64° from ⟨1 0 0⟩ to ⟨1 1 0⟩ in {1 1 0} plane, where Ex 2 was performed 9 days after the Ex 1.

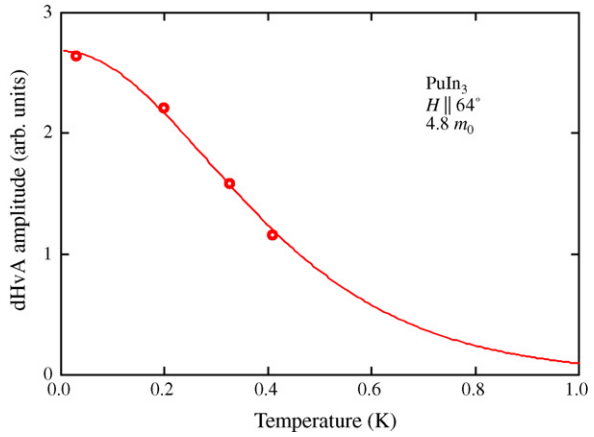

Fig. 6. Temperature dependence of dHvA amplitude in $PuIn_3$. Solid line shows the fit corresponding to the effective mass of 4.8 m_0.

not follow the cubic symmetry. From these experimental results, we conclude that the branch with $F = 5.5 \times 10^6$ Oe is not due to the branch in $PuIn_3$ but due to a dHvA signal of impurities, most likely In, which might be included in sub-grain boundaries of the $PuIn_3$ single crystal sample.

We determined the cyclotron effective mass m_c^* and the Dingle temperature $T_D(= \hbar/2\pi k_B\tau)$ which is inversely proportional to the scattering lifetime τ of conduction electrons, from the temperature and field dependences of the dHvA amplitude A, respectively, as shown shown in Figs. 6 and 7. A relatively large cyclotron mass of $m_c^* = 4.8m_0$ was detected in branch γ from the slope of the mass plot in Fig. 6, where the cyclotron mass of branch with $F = 5.5 \times 10^6$ Oe was not determined, most likely less than 0.5 m_0. This is also the reason why this branch is based on the dHvA signal of In, as mentioned above. The Dingle temperature of branch γ was determined from a slope of the Dingle plot in Fig. 7 as $T_D = 0.87$ K for Ex 1 and $T_D = 1.31$ K for Ex 2. From the relations $S_F = \pi {k_F}^2$, $\hbar k_F = m_c^* v_F$ and $l = v_F\tau$, we can estimate the mean free path of $l = 860$ Å for Ex 1 and 570 Å for Ex 2, where k_F is the Fermi wave number and v_F is the Fermi velocity.

Fig. 8 shows the angular dependence of the dHvA frequency. Branch γ was observed only around ⟨1 1 1⟩. Three solid lines in Fig. 8 indicate the results of 5f-itinerant band calculations. The

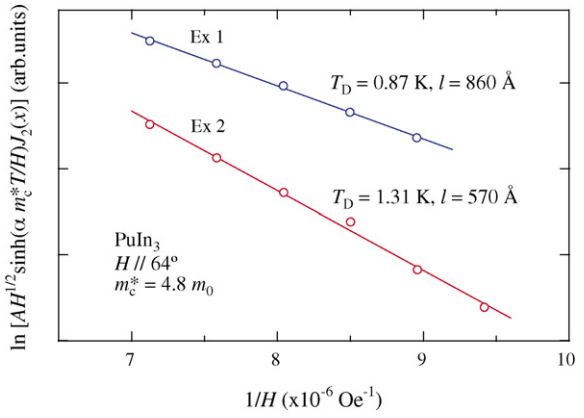

Fig. 7. Dingle plot in $PuIn_3$.

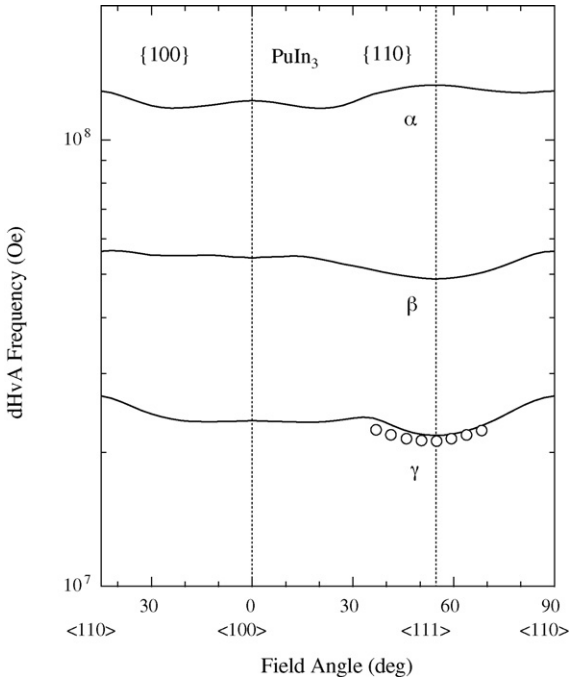

Fig. 8. Angular dependence of dHvA frequency in $PuIn_3$. Solid lines indicate the results of 5f-itinerant energy band calculations.

electronic band calculations are performed using a relativistic linear augmented-plane-wave method [18]. In the iteration procedure, the $5f^5$, $6p^6$, $6d^1$ and $7s^2$ electrons in the Pu site, and the $4d^{10}$, $5s^2$ and $5p^1$ electrons in the In site are treated as valence electrons. The core electrons are considered in the same manner as the self-consistent calculation of atoms. The potentials are defined within the local-density approximation [19]. The experimental lattice parameter is used in the present calculations.

The band calculations predict three kinds of closed electron Fermi surfaces named α, β and γ, as shown in Fig. 9, indicating an uncompensated metal. The Fermi surfaces named α and γ originate from the band-27 electron Fermi surface located at R and Γ points, respectively, while the Fermi surface named β at the R point originates from the band-28 electron Fermi surface. The dHvA frequency of the experimentally obtained branch named γ agrees well with the theoretically obtained band-27 electron Fermi surface located at the Γ point, with the smallest cross-sectional area, as shown in Fig. 8.

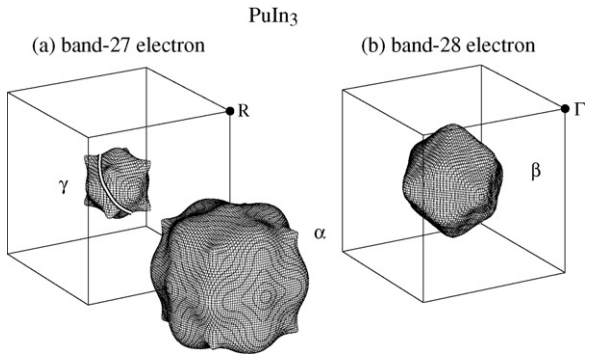

Fig. 9. Three kinds of closed band-27 and 28 electron Fermi surfaces in $PuIn_3$.

Table 1
Theoretical dHvA frequency F, band mass m_b, and curvature factor $|\partial^2 S_F/\partial k_z^2|^{-1/2}$ in $PuIn_3$

	$F(\times 10^7$ Oe)	$m_b(m_0)$	$\lvert\partial^2 S_F/\partial k_z^2\rvert^{-1/2}$
$H \parallel \langle 1\,0\,0\rangle$			
α	12.2	4.42	0.34
β	5.43	2.64	0.29
γ	2.35	1.75	0.48
$H \parallel \langle 1\,1\,0\rangle$			
α	12.8	5.38	0.23
β	5.62	2.49	0.26
γ	2.67	2.06	0.22
$H \parallel \langle 1\,1\,1\rangle$			
α	13.2	3.84	0.27
β	4.88	2.31	0.89
γ	2.18	1.56	0.68

The other two kinds of Fermi surfaces named α and β were not observed experimentally. As shown in Table 1, the band mass of branch γ for $H \parallel \langle 1\,1\,1\rangle$ is the smallest in all the Fermi surfaces and directions, and the curvature factor of $|\partial^2 S_F/\partial k_z^2|^{-1/2}$ in the dHvA amplitude is also preferable for $H \parallel \langle 1\,1\,1\rangle$ compared with other directions. This is the reason why only branch γ was observed around $\langle 1\,1\,1\rangle$. For branch γ, the relative dHvA amplitude for $H \parallel \langle 1\,0\,0\rangle$ based on the parameters in Table 1 and the ratio of the cyclotron mass to the band mass obtained below is estimated to be 0.37. Experimentally, however, no signal was detected for this direction. The reason is not clear.

The detected cyclotron mass of 4.8 m_0 in branch γ is three times larger than the corresponding band mass of 1.56 m_0. A relatively large cyclotron mass of 17 m_0 might be expected for branch α along $H \parallel \langle 1\,1\,0\rangle$. On the basis of the results of the band calculations, the contribution of the 5f component to Fermi surfaces is approximately 50% for branches α and γ, while it is 75% for branch β. Therefore, the ratio of the cyclotron mass to the band mass is expected to be larger in branch β than in branch γ. The electronic specific heat coefficient is estimated as 39 mJ/K^2 mol, using the theoretical value of 12.7 mJ/K^2 mol and the corresponding ratio for branch γ. The difference between the reported electronic specific heat 100 mJ/K^2 mol and the present value might be attributed to the larger contribution from branches α and β which were not observed in the present study.

It is interesting to note that the characteristics of the Fermi surface of $PuIn_3$ are similar to those of an enhanced Pauli paramagnet $YbAl_3$ with the same structure. In the case of plutonium almost five electrons occupy $j = 5/2$ states remaining one hole, while 13 electrons occupy $j = 5/2$ and 7/2 states in $YbAl_3$ [20].

The mean free path of $PuIn_3$ estimated from dHvA effect is only slightly smaller than those of $YbAl_3$ (1100–1500 Å), indicating that the quality of the 'fresh' $PuIn_3$ is as good as $YbAl_3$.

5. Summary

Anisotropic H_{c2} was observed in $PuRhGa_5$ which was explained by the anisotropic mass model. On the other hand, the magnetic susceptibility does not show anisotropy in the paramagnetic region, despite the tetragonal structure.

We have observed dHvA oscillation with an enhanced cyclotron effective mass of a plutonium compound, $PuIn_3$, for the first time. One detected branch named γ corresponds to a band-27 electron Fermi surface based on a 5f-itinerant band model. The detected dHvA amplitude is extremely reduced as a function of time due to point defects produced by α decay of ^{239}Pu.

Acknowledgement

The present work was financially supported by Grant-in-Aid for Scientific Research (A), (C), Creative Scientific Research (15GS0213) from the Japan Society for the Promotion of Science and Scientific Research of Priority Area "Skutterudite" (No. 16037215) from the Ministry of Education, Culture, Sports, Science and Technology.

References

[1] J.L. Sarrao, L.A. Morales, J.D. Thompson, B.L. Scott, G.R. Stewart, F. Wastin, J. Rebizant, P. Boulet, E. Colineau, G.H. Lander, Nature (London) 420 (2002) 297.
[2] F. Wastin, P. Boulet, J. Rebizant, E. Colineau, G.H. Lander, J. Phys.: Condens. Matter 15 (2003) S2279.
[3] N.J. Curro, T. Caldwell, E.D. Bauer, L.A. Morales, M.J. Graf, Y. Bang, A.V. Balatsky, J.D. Thompson, J.L. Sarrao, Nature (London) 434 (2005) 622.
[4] H. Sakai, Y. Tokunaga, T. Fujimoto, S. Kambe, R.E. Walstedt, H. Yasuoka, D. Aoki, Y. Homma, E. Yamamoto, A. Nakamura, Y. Shiokawa, K. Nakajima, Y. Arai, T.D. Matsuda, Y. Haga, Y. Ōnuki, J. Phys. Soc. Jpn. 74 (2005) 1710.
[5] C. Petrovic, R. Movshovich, M. Jaime, P.G. Pagliuso, M.F. Hundley, J.L. Sarrao, Z. Fisk, J.D. Thompson, Europhys. Lett. 53 (2001) 354.
[6] I. Opahle, P.M. Oppeneer, Phys. Rev. Lett. 90 (2003) 157001.
[7] T. Maehira, T. Hotta, K. Ueda, A. Hasegawa, Phys. Rev. Lett. 90 (2003) 207007.
[8] Y. Haga, E. Yamamoto, Y. Tokiwa, D. Aoki, Y. Inada, R. Settai, T. Maehira, H. Yamagami, H. Harima, Y. Ōnuki, J. Nucl. Sci. Technol., Suppl. 3 (2002) 56.
[9] H.R. Ott, Z. Fisk, in: A.J. Freeman, G.H. Lander (Eds.), Handbook on the Physics and Chemistry of the Actinides, Elsevier Science, Amsterdam, 1987 vol. 5, p. 85 (chapter 2).
[10] Y. Haga, D. Aoki, T.D. Matsuda, K. Nakajima, Y. Arai, E. Yamamoto, A. Nakamura, Y. Homma, Y. Shiokawa, Y. Ōnuki, J. Phys. Soc. Jpn. 74 (2005) 1698.
[11] Y. Haga, D. Aoki, H. Yamagami, T.D. Matsuda, K. Nakajima, Y. Arai, E. Yamamoto, A. Nakamura, Y. Homma, Y. Shiokawa, Y. Ōnuki, J. Phys. Soc. Jpn. 74 (2005) 2889.
[12] H. Shishido, R. Settai, D. Aoki, S. Ikeda, H. Nakawaki, N. Kawamura, T. Iizuka, Y. Inada, K. Sugiyama, T. Takeuchi, K. Kindo, T.C. Kobayashi, Y. Haga, H. Harima, Y. Aoki, T. Namiki, H. Sato, Y. Ōnuki, J. Phys. Soc. Jpn. 71 (2002) 162.
[13] J.R. Clem, Physica C 162–164 (1989) 1137.
[14] R. Settai, H. Shishido, S. Ikeda, Y. Murakawa, M. Nakashima, D. Aoki, Y. Haga, H. Harima, Y. Ōnuki, J. Phys. Condens. Matter 13 (2001) L627.
[15] P. Boulet, E. Colineau, F. Wastin, P. Javorsky, J.C. Griveau, J. Rebizant, G.R. Stewart, E.D. Bauer, Phys. Rev. B 72 (2005) 064438.
[16] J.J. Joyce, J.M. Willis, T. Durakiewicz, M.T. Butterfield, E. Guziewicz, D.P. Moore, J.L. Sarrao, L.A. Morales, A.J. Arko, O. Eriksson, A. Delin, K.S. Graham, Physica B 378–380 (2006) 920.
[17] S.S. Hecker, L.F. Timofeeva, in: N.G. Cooper (ed.), Los Alamos Science, No. 26 (2000), p. 244.
[18] H. Yamagami, J. Phys. Soc. Jpn. 67 (1998) 3176.
[19] U. von Barth, L. Hedin, J. Phys. C 5 (1972) 1629.
[20] T. Ebihara, Y. Inada, M. Murakawa, S. Uji, C. Terakura, T. Terashima, E. Yamamoto, Y. Haga, Y. Ōnuki, H. Harima, J. Phys. Soc. Jpn. 69 (2000) 895.